Colloids and Surfaces B: Biointerfaces 208 (2021) 112123

Contents lists available at ScienceDirect

Colloids and Surfaces B: Biointerfaces

journal homepage: www.elsevier.com/locate/colsurfb

Tolerability to non-endosomal, micron-scale cell penetration probed with magnetic particles

Eugènia Ruiz-Cánovas [a,1], Rosa Mendoza [b,a], Antonio Villaverde [a,c,b], José L. Corchero [b,a,c,*]

[a] Institute for Biotechnology and Biomedicine, Universitat Autònoma de Barcelona, Bellaterra, 08193 Barcelona, Spain
[b] CIBER de Bioingeniería, Biomateriales y Nanomedicina (CIBER-BBN), Bellaterra, 08193 Barcelona, Spain
[c] Department of Genetics and Microbiology, Universitat Autònoma de Barcelona, Bellaterra, 08193 Barcelona, Spain

ARTICLE INFO

Keywords:
Magnetic particles
Cell penetration
Cellular therapy
Recombinant protein
Human alpha-galactosidase A

ABSTRACT

The capability of HeLa cells to internalize large spherical microparticles has been evaluated by using inorganic, magnetic microparticles of 1 and 2.8 μm of diameter. In both absence but especially under the action of a magnet, both types of particles were uptaken, in absence of cytotoxicity, by a significant percentage of cells, in a non-endosomal process clearly favored by the magnetic field. The engulfed particles efficiently drive inside the cells chemically associated proteins such as GFP and human alpha-galactosidase A, without any apparent loss of protein functionalities. While 1 μm particles are completely engulfed, at least a fraction of 2.8 μm particles remain embedded into the cell membrane, with only a fraction of their surface in cytoplasmic contact. The detected tolerance to endosomal-independent cell penetration of microscale objects is not then restricted to organic, soft materials (such as bacterial inclusion bodies) as previously described, but it is a more general phenomenon also applicable to inorganic materials. In this scenario, the use of magnetic particles in combination with external magnetic fields can represent a significant improvement in the internalization efficiency of such agents optimized as drug carriers. This fact offers a wide potential in the design and engineering of novel particulate vehicles for therapeutic, diagnostic and theragnostic applications.

1. Introduction

Intracellular drug delivery is on the basis of precision medicines. Capability to drive the controlled internalization in target cells of materials with therapeutic potential has been explored by a wide spectrum of nanomedical approaches [1]. The use of cell-penetrating peptides for a fast and efficient internalization or of ligands of cell surface molecules acting as selective receptors [2] is accompanied by the development of appropriate nanocarriers for payload drugs and/or imaging agents [3]. In a prototypic nanoconjugate, a nanoscale vehicle is functionalized with such peptides and chemically coupled or loaded with the cargo [4,5].

Multiple materials and vehicle types are being explored as drug delivery systems (DDS), as well as different sizes, geometries and surface charges of the final conjugates. Among them, nano- and micro- particles with magnetic properties (MPs) are increasingly being used in a wide spectrum of biomedical applications. After functionalization to enable specificity, MPs can be conveniently positioned both in vitro and in vivo using magnetic fields. Moreover, after reaching their targets, MPs exposure to a high frequency alternating magnetic field (AMF) results in a localized temperature increase in target cells (hyperthermia) by MPs activation, inducing localized cell death. Such properties have shown a significant therapeutic value in, for instance, cancer therapy. Other promising biomedical applications for MPs include magnetically enhanced transfection (magnetofection), biomolecules purification, gene therapy, or tissue engineering, among others [6,7].

Once at the target location, DDS face cellular uptake, an essential event required to deliver their therapeutic cargo. Apart from other relevant physicochemical parameters, there is a consensus in the fact that size determines both nanovehicle fate and its cell uptake. Even within the nano-scale range, particle size strongly affects bioavailability and blood circulation time [8,9]. Following systemic administration, nanoparticles with diameters below the renal cut-off (approx. 7–8 nm) are rapidly eliminated through extravasation and renal clearance [10]. A nanoscale size over 10 nm prevents renal clearance and also benefits from the enhanced permeability and retention (EPR) effect, if the drug is

* Corresponding author at: Institute for Biotechnology and Biomedicine, Universitat Autònoma de Barcelona, Bellaterra, Barcelona 08193, Spain.
E-mail address: jlcorchero@ciber-bbn.es (J.L. Corchero).
[1] Present address: GAT Therapeutics SL, Parc Científic de Barcelona, C/ Baldiri Reixac 4–8, 08028 Barcelona, Spain.

https://doi.org/10.1016/j.colsurfb.2021.112123
Received 5 February 2021; Received in revised form 11 September 2021; Accepted 16 September 2021
Available online 20 September 2021

intended for oncology. Usually, optimal sizes for cell penetration have been determined to be between 20 and 80 nm, with some variability depending on the experimental setting up. Particles with such size ranges can penetrate even very small capillaries [11] and ensure smooth endosomal-mediated cell penetration as well as the maintenance of cell integrity and viability during the process. Particles with diameters ranging from 70 to 200 nm demonstrate the most prolonged circulation times [8], while particles with diameters greater than 200 nm are usually sequestered by the spleen and eventually removed by phagocytes [12].

Interaction of nanoparticles with the cell membrane plays a key role in the internalization mechanics [13–16], which consequently impacts in the efficiency of the process or application, such as biomedical imaging and drug delivery. Two important steps of these processes are the adhesion of the particles to the membrane and their subsequent engulfment. Recently, we have demonstrated that a special type of proteinaceous material, namely bacterial inclusion bodies (IBs), can penetrate mammalian cells in absence of toxicity [17–24]. Being a soft matter, IBs are mechanically stable protein clusters that, in form of functional non-toxic amyloids, show a size range between 0.5 and 1 μm. The penetration of bacterial IBs into mammalian cells seems to be favored by a strong membrane affinity shown by such protein materials, but it can be additionally targeted to specific cell receptors by incorporating appropriate ligands of cell surface receptors [23,25–27]. The same penetrability in absence of toxicity has been very recently demonstrated for artificial IBs, IB mimetics generated in vitro but showing a diameter ranging between 2 and 3 μm [28–30]. When either IBs or artificial IBs contain a protein with therapeutic value, target cells benefit from such biological activity, demonstrating, in a functional way, the efficient internalization of the material [31–33].

Irrespective of the mechanisms that allow cell penetration of micron-scale materials, still not completely solved, this possibility is promising, as it would largely increase the drug delivery potential of particulate systems. However, it is not clear if the cell penetrability described for IBs is linked to their soft matter nature, or to other particular properties such as membrane avidity. Therefore, a better understanding of the mechanisms involved in the cell uptake processes could help in the future to increase the delivery efficiency of therapeutic compounds by micron particles. In this context, we have tested here the tolerance of cultured cells to the penetration of large microparticles, by using a hard, inorganic material system based on magnetic particles. The obtained data reveal a cell tolerability higher than expected regarding the size of particulate materials than cells can uptake, in absence of any detectable cytotoxicity. The results are discussed under the light of potential novel applications of these new concepts in drug delivery and imaging.

2. Material and methods

2.1. Magnetic particles (MPs)

Commercial Dynabeads® MyOne™ Tosylactivated (ref. 655.01, 1 μm diameter), M-280 Tosylactivated (ref. 301.01, 2.8 μm diameter) and Dynabeads® TALON™ (ref. 101.01, 1 μm diameter) were obtained from Dynal® (Invitrogen). Tosylactivated particles are polystyrene beads coated with a polyurethane layer. The hydroxy groups are activated by reaction with p-toluensulphonyl chloride. The resulting sulphonyl ester can react covalently with the amino groups present in the cargo protein. Thus, any ligand (e.g. antibody, protein, peptide or glycoprotein) containing amino groups can be covalently coupled to the beads surface. Tosylactivated MyOne and M-280 magnetic particles do not need additional activation prior to protein immobilization procedures, and their handling and protein coupling was done according to the manufacturer instructions. Dynabeads® TALON™ MPs use cobalt-based Immobilized Metal Affinity Chromatography (IMAC) using magnetic beads on which the BD TALON™ chemistry has been immobilized. The TALON technology is based on a tetradentate metal chelator in which four of cobalt's six coordination sites are occupied. The imidazole rings of histidine residues present in a 6xHis tag are able to occupy the two remaining coordination sites, resulting in protein binding.

Magnetic particles were magnetically captured either with a magnetic rack (New England Biolabs, rack S1506S) or with a precision magnetophoresis system from Sepmag Systems (STEPMAG 125).

2.2. Recombinant proteins used as "cargo" attached to magnetic particles

Two recombinant proteins (with either fluorescent or enzymatic properties) were coated onto the different magnetic particles and used as a cargo to check the ability of these magnetic vehicles to deliver a protein to a target cell. A 6xHistidine-tagged recombinant green fluorescence protein (GFP-H6) was produced in Rosetta BL21(DE3) *Escherichia coli* as previously described [34]. As a second model protein, a 6xHistidine-tagged human alpha-galactosidase A (GLA) was chosen. The enzymatic activity of GLA enzyme can be easily determined by in vitro assays and, in addition, it has therapeutic value, functioning here as a model of a protein drug. Its deficiency causes Fabry disease, a rare pathology currently treated by periodic administration of the recombinant enzyme. Recombinant GLA used here was produced by PEI-mediated transient gene expression in mammalian HEK 293F cells as previously described [35]. Both GFP and GLA proteins were purified by affinity chromatography using HiTrap Chelating HP columns (GE Healthcare) following the manufacturer instructions. In some experiments, a commercial bovine serum albumin (BSA, bovine serum albumin fraction V, Roche, ref. 001,10,078,735) was used as a negative control (protein without fluorescence or enzymatic activity).

2.3. Conjugation of proteins to magnetic particles

Tosylactivated (M-280 and MyOne) particles were coated as previously described [36]. Briefly, particles to be GLA-coated (10 mg unless otherwise stated) were washed twice with coating/storage buffer (0.01 M acetic acid, pH 4.5) and resuspended in the same buffer with 200 μg/ml GLA (20 μg GLA/mg particles). After conjugation (overnight, in agitation at 25 rpm, 37ºC), particles were magnetically captured, and the supernatant removed. Coated particles were then washed for 15 min with phosphate buffered saline (PBS) plus Tween-20 0.05% (in order to remove only-adsorbed, non-covalently attached protein), for 15 min with 0.2 M Tris-HCl pH = 8 (to block the remaining free tosyl groups), and twice with PBS. Finally, they were diluted in coating/storage buffer to 1.5 mg MPs/ml and kept at 2–8 ºC. For GFP-His and BSA coating, protocol was essentially the same, but using PBS instead of acetic acid as coating/storage buffer. On the other hand, TALON MPs were coated with GLA enzyme as follows. After washing with PBS, particles were diluted in PBS with 200 μg/ml of protein (20 μg protein/mg particles). After protein capture (in agitation at room temperature for 30 min, as recommended by the supplier), supernatant was removed. MPs were washed 4 times with PBS, diluted in PBS to 1.5 mg MPs/ml and stored at 2–8 ºC.

2.4. Cell culture, magnetic-driven internalization studies and particles cytotoxicity

HeLa cells (human cervical carcinoma, from the American Type Culture Collection, reference CCL-2) were grown as monolayers in Dulbecco's modified Eagles's medium (DMEM) with 50 units/ml penicillin, 50 μg/ml streptomycin, and supplemented with 10% fetal bovine serum (FBS). Cell cultures were performed in a 5% CO_2 humidified atmosphere at 37ºC.

For internalization experiments, cells were seeded into two 24-well plates at an initial density of 50,000 cells/well. Cells exposure to magnetic particles was performed 24 h after plating, at approximately 60–70% cell confluence. Before exposure to magnetic particles, cell culture supernatants were removed and replaced by 500 μL of fresh

medium. One plate was kept as a "Control" and the other ("Magnet plate") was placed over a BioMag® Flask Separator (Bangs Laboratories, Inc., ref. MS004). The BioMag® Flask Separator is a 12.5 cm × 6 cm rectangular magnetic separation unit designed for use with tissue culture flasks or plates. The unit consists of 24 permanent magnets encased in a plastic frame. The magnetic strength for each disc magnet is 27 megagauss Oersteds. Then, cells and magnetic particles were incubated together (at room temperature) in both "Control" and "Magnet" plates, by adding at different time-points 25 μL of protein-coated MPs to the corresponding wells. After incubation, magnet was removed, and supernatants from both plates were gently aspirated. Cells were washed twice with 500 μL of cold PBS, and trypsinized with 500 μL of trypsin 0.05%, during 10 min at 37ºC. Then, cells were transferred to microcentrifuge tubes, centrifuged at 1500 rpm for 10 min, supernatant was discarded, and cells were resuspended in 1 ml of PBS. After that, percentage of fluorescent cells was determined by flow cytometry (FACSCalibur, BD Biosciences, San José, CA). This protocol is schematically outlined in Fig. 1. In the case of internalization of GLA-coated particles, protocol was essentially the same, but with the following modifications: after internalization and washing, cells were resuspended in 500 μL of distilled H_2O, gently sonicated, and lysates were directly submitted to the GLA enzymatic assay.

For cytotoxicity studies, protein-coated MPs were added to cells as previously described. Internalization of MPs was magnetically driven by 10 min incubation with the magnet. Then, cells were washed, and fresh medium was added. After 24 h of incubation, cell viability was estimated with the EZ4U Cell Proliferation and Cytotoxicity Assay (Biomedica, ref. BI-5000), a cell proliferation and cytotoxicity assay based on the reduction of tetrazolium salt to colored formazan.

2.5. Confocal microscopy analysis

For confocal analysis, cells were grown to 100,000 cells/ml on MatTek culture dishes (MatTek Corporation) for 24 h at 37 °C at 5% CO_2. Incubation with MPs was done as previously described, but without the final trypsinization step. Then, and before confocal observation, cell nuclei were labeled with 5 μg/ml Hoechst 33342 (Life Technologies) and plasma membranes with 2.5 μg/ml CellMask™ Deep Red (Life Technologies) for 10 min in the dark. Micrographs were then taken by TCS-SP5 confocal laser scanning microscopy (Leica Microsystems) using a Plan Apo 63 × /1.4 (oil HC × PL APO lambda blue) objective. Z-series were collected at 0.5 mm intervals, and images processed using Imaris version 6.1.0 software (Bitplane, Zürich, Switzerland). Z-stack function was applied. Multiple images were taken along the z-direction to study the cells in depth. The in-depth imaging allowed the cells and MPs interactions to be visualized in 3-dimensions. This was used to figure out whether the MPs were completely internalized, just next to the cell or membrane embedded.

2.6. Enzymatic assay of GLA activity

Enzymatic GLA activity was assayed fluorometrically as described by Desnick et al. [37] with the modifications of Mayes et al. [38] Basically, enzymatic GLA activity was assayed with 4-methylumbelliferyl α-D-galactoside (4-MUG, ref. M7633, Sigma Chemical) as substrate, at a concentration of 2.46 mM in 0,01 M acetic buffer (pH 4.5). A typical assay was performed with a reaction mixture containing 100 μL of substrate and 25 μL of cells lysates. Enzymatic reactions took place in agitation, at 37ºC for 1 h, followed by their termination by addition of 1.25 ml of 0.2 M glycine-NaOH buffer (pH 10.4). The released 4-methylumbelliferone (4-MU) was determined by fluorescence measurement at 365 and 450 nm as excitation and emission wavelengths, respectively. Samples ranging from 5 to 500 ng/ml of 4-MU (ref. M1381, Sigma, St. Louis, MO) in 0.2 M glycine-NaOH buffer (pH 10.4), were used to calibrate the readings. Results are expressed as ng 4-MU/ml.

2.7. Statistical analysis

The quantitative data of the experiments is reported as mean ± standard error of the mean (SEM). Pairwise comparisons between

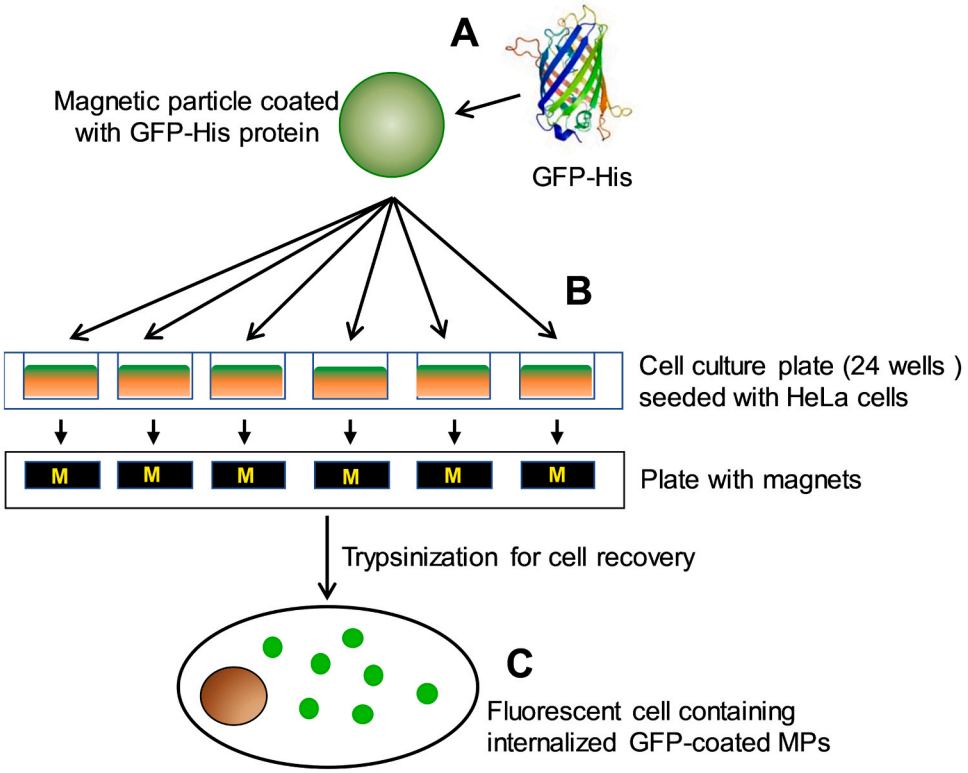

Fig. 1. General strategy to deliver MP-coated proteins into cells. A: MPs are coated with a protein (e.g. GFP) as described in Materials and Methods. B: Coated MPs are added to the wells and forced to enter into HeLa cells by exposure (during different times) to magnetic force, by contact with magnets placed under the cell culture plate. C: After magnetic exposure, cells are washed, trypsinized and recovered. By flow cytometry, the percentage of fluorescent cells (due to previous uptake of fluorescent MPs) is determined.

groups were determined by paired *t*-test with Excel software (Microsoft Corporation). Probability values (p) < 0.05 were regarded as statistically significant, and relevant divergences were labeled as $*p < 0.05$, $**p < 0.01$ and $***p < 0.001$.

3. Results and discussion

Initially, internalization of GFP-coated MPs of two different diameters (1 and 2.8 μm) in cultured HeLa cells was checked, using a magnet to force MPs to contact and penetrate into the cells. Initially, GFP was covalently attached to MPs by the tosyl groups present in MPs surface and was used as a convenient reporter of internalization but also as a model of a potentially attached drug, imaging or any other functional agent, to evaluate its stability during the process.

In absence of a magnetic force, 1 μm nanoparticles are able to spontaneously penetrate within a significant fraction of cultured cells, resulting in ~10% of fluorescent cells after 30 min of exposure (Fig. 2, left panel). A smaller, but still detectable fraction of cells becomes fluorescent when exposed to 2.8 μm particles (Fig. 2, right panel). In this case, the bigger particle size clearly hampers their spontaneous internalization without the external aid of the magnetic force. Interestingly, cell exposure to 1-micron particles in absence of magnetic force for more than 30 min does not result in better percentage of internalization, but it results in a slight decrease in the final percentage of fluorescent cells. This effect is not evident for 2.8 μm MPs, most probably due to the very low levels of internalization observed under these experimental conditions.

On the other hand, when a magnetic field is applied, MPs are forced to enter cells, reaching a peak of fluorescent cell population after 5 or 10 min of exposure to 1 μm and 2.8 μm MPs, respectively. In this line, and for both MPs types, percentages of fluorescent cells with or without the magnetic field are statistically different, corroborating the positive effect of the magnetic field in MPs internalization. Moreover, the magnetically mediated penetration of 1 μm nanoparticles is faster and slightly more efficient than those of larger ones, as well as their apparent stability or permanence inside cells. In a previous study, barium sulphate nanoparticles with three different sizes (40 nm, 420 nm, and 1 mm) were all efficiently taken up by bone marrow-derived phagocytosing cells (bmPCs) within a few hours. The amount of uptaken nanoparticles increased with increasing particle concentration in the medium and with increasing incubation time [39]. In contrast, using magnetic materials as DDS, in combination with an appropriate magnetic force, could greatly decrease the time needed to interact and enter target cells. This shows a clear advantage of magnetic vehicles over other types of DDS. The decreasing fraction of cells with intracellular material, observed when increasing the magnetic exposure longer than 10–15 min, is probably indicative of a transient intracellular lastingness of the materials in presence of a constant unidirectional magnetic field, which might also remove the particles from cells. The fact that the fluorescent fading is softer in absence of the magnet fully supports this hypothesis, that we would favor over an intracellular degradation of the cargo protein once inside the cells, that is presumed to require longer times.

To assess if the fluorescence emitted by cells is due to a real internalization of MPs instead of a mere cell surface anchorage, confocal microscopy images of cells exposed to both types of MPs for 10 min were obtained (Fig. 3).

Most of the smaller MyOne-GFP particles were detected inside the cells, clearly separated from cell membrane (left panels). The uptake was confirmed by 3D reconstructions (left, upper panel) and the lateral projections (left, lower panel), that rendered images compatible with the full uptake of the material. On the other hand, M280-GFP particles (right panels) were mainly found on the cell surface, embedded in the cell membrane but not being fully engulfed. Lateral projections revealed a fraction of the particles remaining exposed to the media and other areas partially internalized and facing the cell cytoplasm. In this respect, it has been reported that a greater cellular association of paclitaxel into 4T1, Caco-2, and Cor-L23/R cells was achieved when delivered in microparticles compared to nanoparticles [40]. There, authors hypothesized that larger microparticles adhere to mucus on the cell surface, enhancing the cellular association of paclitaxel. In a more recent study, further experiments supported the hypothesis that microparticles adhere to, and are retained in the mucus on the cell surface, and are not internalized by clathrin-mediated endocytosis or macropinocytosis [41]. This fact unexpectedly indicates that the cell penetration previously described for soft protein materials, as bacterial IBs or their biomimetic particles, is not restricted to soft materials, but it seems to be a general event. Interestingly, these visualizations are compatible with the observation of HeLa cells exposed to GFP IBs that were also, in some cases, partially internalized and tightly attached to the cell membrane [22]. The process by which bacterial IBs interact with mammalian cells has been recently explored. Such process starts with an early and tight cell membrane anchorage of IBs, followed by cellular uptake of single or grouped IBs of variable sizes by micropinocytosis. Despite the high affinity of IBs for cell membranes, the first completely internalized particles were not observed by TEM until 3 h after their addition to cell cultures. At longer incubation times, a significant number of IBs could be detected completely inside the cells in periods of time significantly shorter than those described in previous studies [19,21,22,32].

In the context of such deep interaction but partial internalization observed for large particles, we decided to evaluate the availability to exposed cells of a functional protein (other than GFP) linked to the magnetic, inorganic materials. For that, a recombinant human alpha-galactosidase A (GLA, a lysosomal enzyme with therapeutic uses in

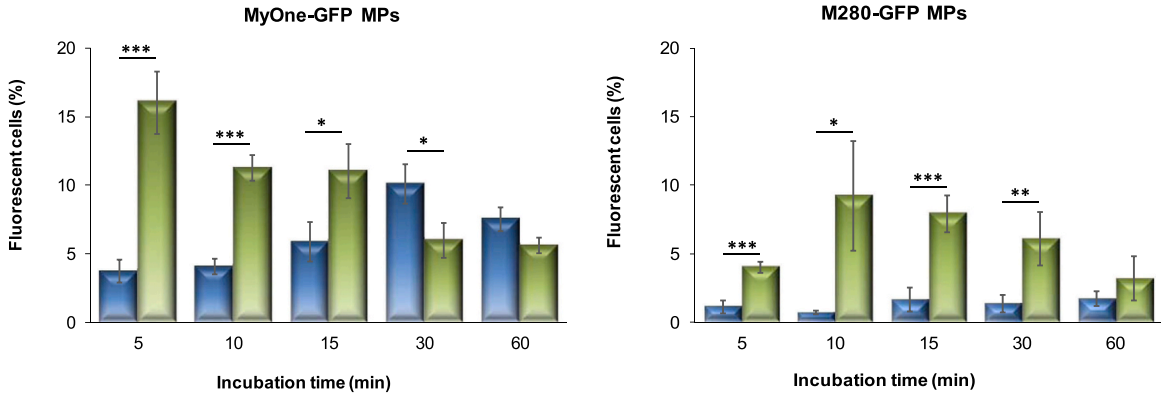

Fig. 2. Effect of MPs diameter in their magnetically mediated entrance within HeLa cells. Left: MyOne particles (1 μm diameter). Right: M280 particles (2.8 μm diameter). Percentages of fluorescent cells after different incubation times in the absence (blue bars) or presence (green bars) of magnet are shown. Values are given as mean and SEM of duplicates for each condition and time tested, performed in 3 independent experiments.

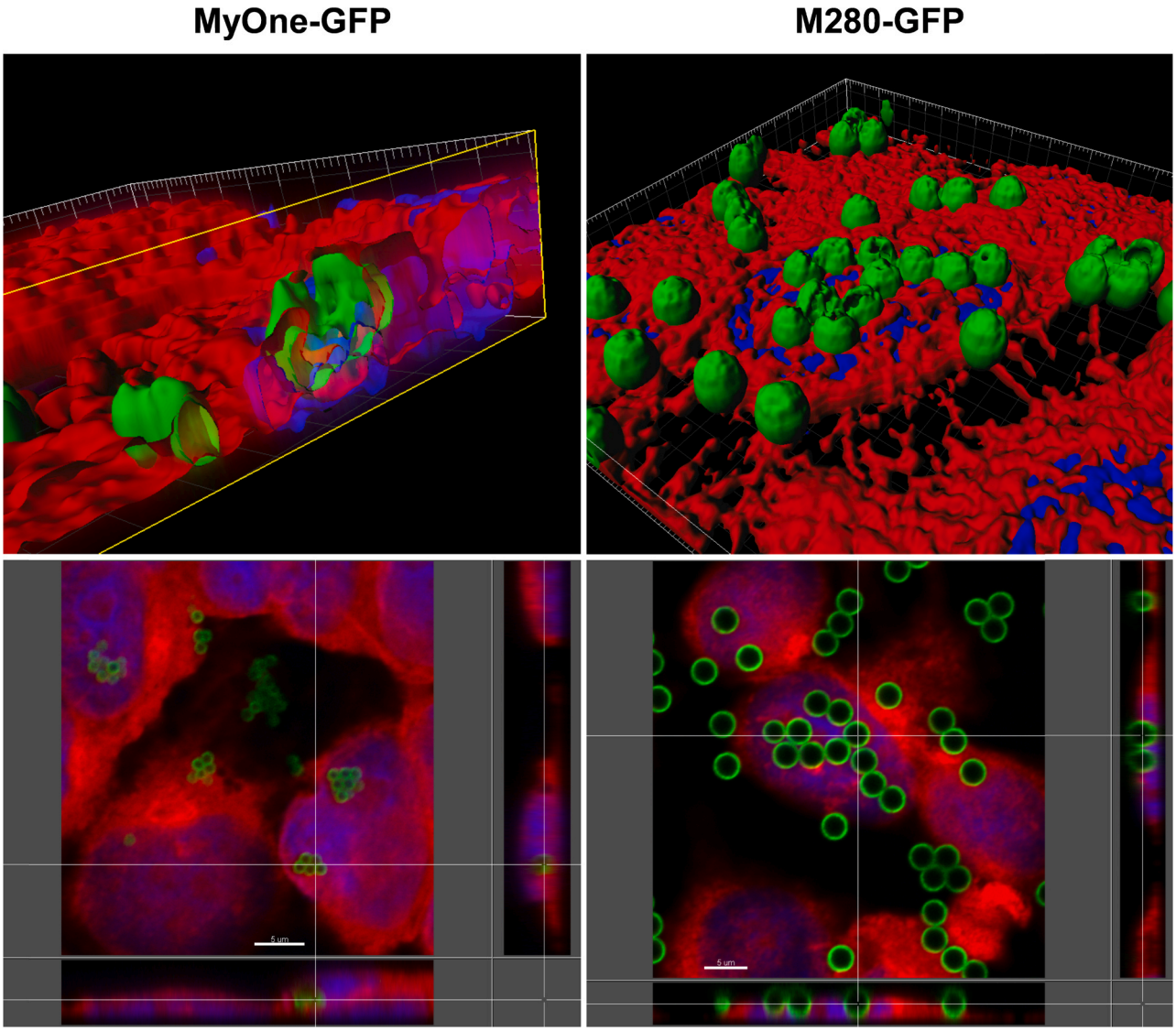

Fig. 3. Internalization of GFP-coated MPs in HeLa cells, by confocal microscopy. Left panels: MyOne-GFP particles. Right panels: M280-GFP particles. Bar: 5 μm.

enzyme replacement therapy) [42], was selected as payload. Fabry disease is an X-linked disease characterized by the accumulation of globotriaosylceramide (Gb3) and other glycosphingolipids in cellular lysosomes, caused by a deficient activity of the GLA enzyme. Enzyme replacement therapy (ERT) was the first disease-specific treatment for Fabry patients, providing a clear therapeutic benefit [43]. Nowadays, recombinant GLA-based ERT remains the main treatment for most Fabry patients. Moreover, GLA enzyme might have interesting applications in other fields, like in the food industry. There are several reports on the use of GLA from plants [44], bacteria [45], yeast [46] and fungal sources [47] for the removal of raffinose family sugars (major factors responsible for flatulence due to soybean and legumes ingestion). GLA is also known to remove galactose moieties from guar (*Cyamopsis tetragonoloba*) gum, improving its gelling properties, and GLA-modified galactomannan has been used to improve the gelling properties of some polysaccharides [48]. In a more biomedical field, GLA has shown a very appealing application in blood transfusion by removing the immunodominant α-1,3-linked galactose residues from group B red blood cells [49–51]. In this context, enzymatic conversion of group B red blood cells using purified or recombinant coffee bean GLA has already been achieved [52,53], eventhough the high amounts of enzyme needed constituted an economic obstacle for routine use in blood transfusions.

Moreover, in a previous work we explored different procedures and chemistries to coat GLA enzyme onto different TALON and tosyl-based MPs, and the effects of such immobilization process in both structural and enzymatic GLA parameters [36]. GLA enzyme could be successfully immobilized by means of alternative coupling chemistries (covalent and metal affinity adsorption), and results showed that such immobilized GLA had higher specific activity and enhanced stability than its soluble counterpart, as well as the possibility of reusability due to the immobilization process. TALON chemistry seemed to provide better results in terms of better GLA specific enzymatic activity, suggesting a clear influence of the chemistry used for immobilization on the final structure and performance of the enzyme. GLA enzyme is mainly attached to the TALON MPs surface by its C-terminal hexahistidine tag, rendering a more homogeneous, well-ordered disposition of the protein onto the surface. On the contrary, for tosyl-activated MPs (MyOne and M-280), any amino group (either at the N-terminus or in the lateral chains of any solvent-exposed amino acid residue) exposed at the protein surface can be theoretically covalently coupled to the tosyl groups present in MPs. This means that GLA can be covalently attached to the surface by several different amino groups present at its surface, therefore acquiring different conformations (some of them being more favorable than others to the enzymatic reaction). These two strategies of GLA coupling are outlined in Fig. 4.

Improvement of key characteristics like specific activity and/or

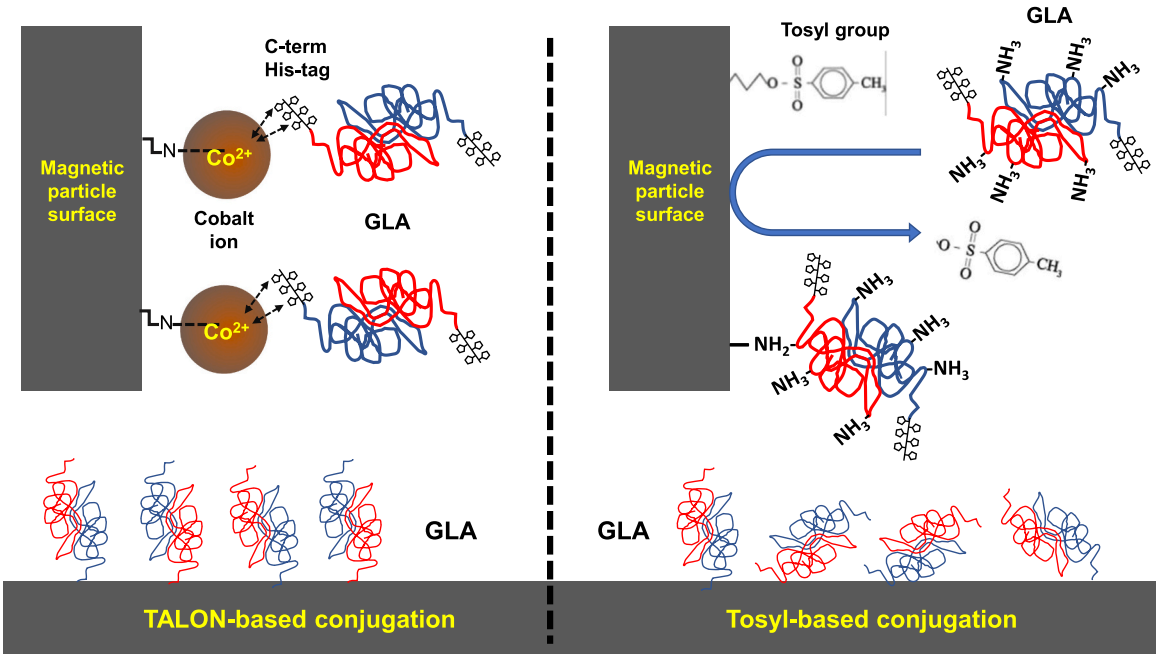

Fig. 4. Influence of coupling strategies in the final disposition of GLA molecules onto MPs surface. The TALON technology (left side) is based on a tetradentate metal chelator in which four of cobalt's six coordination sites are occupied. The imidazole rings of histidine residues present in the His-tag occupy the two remaining coordination sites, resulting in protein binding. Thus, GLA enzyme is mainly coupled to TALON MPs surface by its C-terminal His-tag, rendering a more homogeneous, well-ordered disposition of the protein onto the surface. On the other hand, tosyl groups (right side) can react covalently with any amino group present in the cargo protein. This means that GLA can be covalently attached to the surface by several different amino groups present at its surface, therefore acquiring different conformations.

thermal stability after enzyme immobilization is not exclusive of GLA. On the contrary, protein immobilization seems to result, as a general trend, in a stabilization of the protein structure and therefore a better biological performance. This has been already described for different proteins, like glycosyltransferases [54], antibodies [55], alkaline phosphatase [56], amyloglucosidase [57], or α-chymotrypsin [58]. All these results together make magnetic bioconjugates excellent platforms to display highly active versions of human GLA for both in vitro catalysis and therapeutic applications.

In this context, we first tested the ability of M-280 MPs to deliver enzymatically active GLA into HeLa cells. As a control, no MPs and M-280 MPs coated with irrelevant proteins (GFP and BSA) were included.

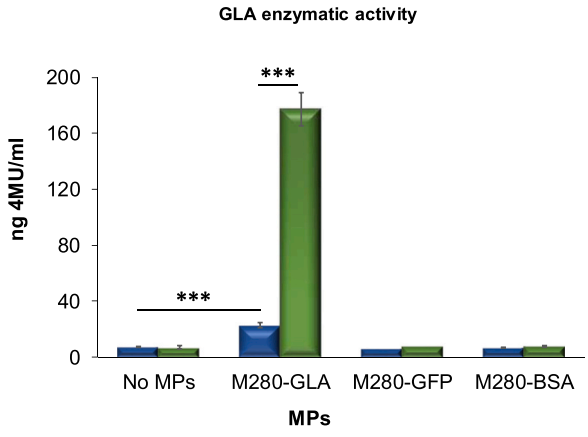

Fig. 5. Delivery of GLA enzyme by means of M-280 MPs. M-280 particles coated with different proteins (GFP, GLA or BSA) were incubated with HeLa cells for 5 min in the absence (blue bars) or presence (green bars) of magnet. Then, cells were recovered by trypsinization, lysed and submitted to the GLA enzymatic assay. Values are given as mean and SEM of at least 4 independent samples.

As shown (Fig. 5), cells treated with GLA-coated MPs showed a significant intracellular GLA enzymatic activity, as trypsinization is expected to remove externally attached enzyme. As presumed, only background GLA activity was detected in HeLa cells treated with M280-GLA MPs but not submitted to magnetic force. Such residual GLA activity cannot be explained by the action of endogenous GLA, since cells not treated or treated with control MPs did not show any background value. In this line, such GLA activity is statistically higher than that found in cells not confronted to MPs. On the other hand, intracellular levels of GLA activity were clearly enhanced when the magnetic force was applied. This result was indicative of the bioavailability of the enzyme even under the partial penetration of such larger particles suggested by confocal 3D reconstructions (Fig. 3).

In a further experiment (Fig. 6), the kinetics of intracellular GLA

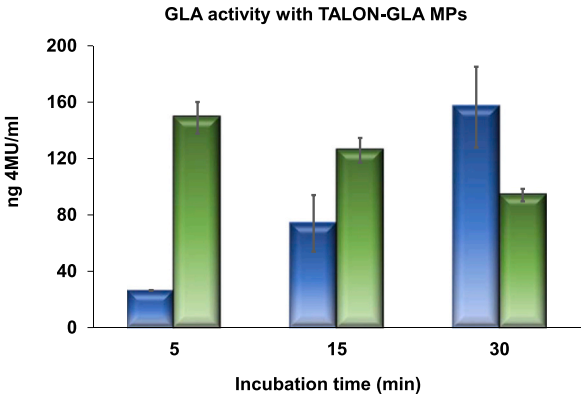

Fig. 6. Delivery of GLA enzyme by means of TALON particles coated with GLA. TALON-GLA MPs were incubated with HeLa cells for different times in the absence (blue bars) or presence (green bars) of magnet. Then, cells were recovered, lysated and submitted to the GLA enzymatic assay. Values are given as mean and SEM of two independent samples.

activity was monitored in GLA-loaded TALON microparticles (1-micron diameter). These MPs allowed spontaneous, time-dependent entrance into cells in the absence of a magnet at levels comparable to those of larger particles. On the other hand, the use of a magnet significantly accelerated MPs entrance as well as the transient nature of the intracellular permanence, as indicated by data shown in Fig. 2. Again, the levels of internalized GLA were similar to those reached by larger MPs in presence of the magnet.

To fully confirm such membrane flexibility, we performed an analysis of cytotoxicity potentially caused by all types of used MPs. As observed (Fig. 7), none of the used MPs caused a significant decrease in cell viability when compared to untreated cells, or to cells exposed to MPs storage buffers (PBS pH 7.4, or acetic acid pH 4.5).

4. Conclusion

Microparticles, and specially nanoparticles, have been extensively explored as drug delivery systems. However, success of such vehicles relies on the ability to overcome two main key bottlenecks in the administration pathway, namely a poor biodistribution through an appropriate site-specific cell targeting, and the external localization of the drug, through an efficient cellular uptake of the drug-material conjugates. In this sense, magnetic vehicles are very attractive for the delivery of therapeutic agents as they can be targeted to specific locations in the body through the application of a magnetic field gradient. Such ability has been explored in processes like magnetofection or hyperthermia therapy. However, once the target cell has been reached, successful applicability of nano- and microparticles as DDS depends, among other factors, on their ability to bind to and cross cell membranes. Proteins are generally unable to cross the membrane barrier of eukaryotic cells. Thus, interaction of the drug carrier (nano- and microparticles) with cell membranes is of paramount importance. Two main steps of this interaction between vehicle and membrane are the adhesion of the particles to the membranes and their subsequent engulfment by these membranes.

The capability of large magnetic particles to intracellularly deliver cargo proteins in a functional way, demonstrated in this study, opens a plethora of possibilities regarding the use of hard materials as vehicles for cell internalization. The control of the particle size in the range 1–2.8 μm allows to determine the localization of the material upon the application of magnetic fields. While smaller particles penetrate with high efficacy, most of the larger particles remain associated to the outer side of the cell membrane, or deeply embedded in the lipidic bilayer. Such a discrimination cannot be achieved by conventional homing materials such as nanoparticles functionalized with peptidic ligands of cell surface molecules, that inexorably determine the endosomal route of cell penetration. Interestingly, the engulfment of MPs with or without payload, as driven with a magnet, does not result in any loss of cell viability or in morphological aberrations of the target cells. We have proved that large MPs used as internalizing drug carriers are fully biocompatible, as determined by a cell viability assay, and under the conditions tested in this study, some of them quite harsh and intrinsically challenging cell viability.

The membrane-linked localization of larger materials would be especially appealing to deliver hormones, growth factors, antagonists and other cell signaling effectors with complicated delivery processes. In any case, solving the potentiality of large and hard micro-scale materials to be delivered into target cells allows considering them as potential alternatives for drug delivery that, unlike soft material such as proteins, admit extensive chemical modifications to reach complex, on-demand functionalities in drug delivery.

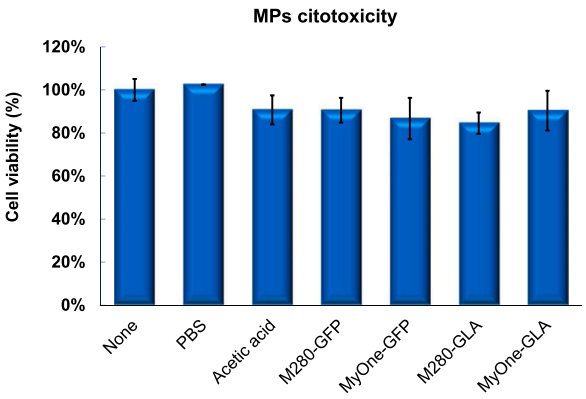

Fig. 7. Cytotoxicity of MPs. M-280 and MyOne particles coated with different proteins (GFP or GLA) were incubated with HeLa cells for 10 min in the presence of magnet. Then, cells were washed and incubated 24 h in fresh medium. Finally, cells were submitted to the MTT metabolic assay. Values are given as mean and SEM of at least 3 independent samples.

Funding sources

We acknowledge financial support to our research received from Instituto de Salud Carlos III, through "Acciones CIBER". The Networking Research Center on Bioengineering, Biomaterials, and Nanomedicine (CIBER-BBN) is an initiative funded by the VI National R&D&I Plan 2008–2011, Iniciativa Ingenio 2010, Consolider Program, CIBER Actions and financed by the Instituto de Salud Carlos III with assistance from the European Regional Development Fund. We are indebted to AGAUR (2017SGR-229, to AV). AV received an ICREA ACADEMIA award.

CRediT authorship contribution statement

Eugènia Ruiz-Canovas: Investigation, Data curation. **Rosa Mendoza**: Investigation. **Antonio Villaverde**: Conceptualization, Supervision, Writing – review & editing. **José L. Corchero:** Conceptualization, Investigation, Supervision, Data curation, Writing – original draft, Writing – review & editing.

Declaration of Competing Interest

The authors declare that they have no known competing financial interests or personal relationships that could have appeared to influence the work reported in this paper.

Acknowledgments

We thank Dr. Lluís M. Martínez and Sepmag Systems for their technical help and kindly providing the Stepmag 125 magnetic separation system, and to Dr. Escarlata Rodríguez-Carmona for their support and technical help regarding protocols for magnetic particles coating. Cell culture experiments and confocal microscopy analysis were performed at the Cell Culture Service (SCAC) and at the Servei de Microscòpia (both at the UAB), respectively. We also acknowledge the ICTS "NANBIOSIS", more specifically the support from the Protein Production Platform of CIBER-BBN/IBB, at the UAB SepBioES scientific-technical service (http://www.nanbiosis.es/unit/u1-proteinproduction-platform-ppp/).

References

[1] B. Fluhmann, I. Ntai, G. Borchard, S. Simoens, S. Muhlebach, Nanomedicines: the magic bullets reaching their target? Eur. J. Pharm. Sci. 128 (2019) 73–80.
[2] K. Kardani, A. Milani, H. Shabani, A. Bolhassani, Cell penetrating peptides: the potent multi-cargo intracellular carriers, Expert. Deliv. 16 (2019) 1227–1258.
[3] S. Su, M. Kang, Recent advances in nanocarrier-assisted therapeutics delivery systems, Pharmaceutics. 12 (2020) 837.
[4] A.H. Azandaryani, S. Kashanian, T. Jamshidnejad-Tosaramandani, Recent insights into effective nanomaterials and biomacromolecules conjugation in advanced drug targeting, Curr. Pharm. Biotechnol. 20 (2019) 526–541.

[5] R. Lehner, X. Wang, S. Marsch, P. Hunziker, Intelligent nanomaterials for medicine: carrier platforms and targeting strategies in the context of clinical application, Nanomedicine. 9 (2013) 742–757.

[6] J.L. Corchero, A. Villaverde, Biomedical applications of distally controlled magnetic nanoparticles, Trends Biotechnol. 27 (2009) 468–476.

[7] A. Hasan, M. Morshed, A. Memic, S. Hassan, T.J. Webster, H.E. Marei, Nanoparticles in tissue engineering: applications, challenges and prospects, Int. J. Nanomed. 13 (2018) 5637–5655.

[8] O. Ishida, K. Maruyama, K. Sasaki, M. Iwatsuru, Size-dependent extravasation and interstitial localization of polyethyleneglycol liposomes in solid tumor-bearing mice, Int. J. Pharm. 190 (1999) 49–56.

[9] G. Kong, R.D. Braun, M.W. Dewhirst, Hyperthermia enables tumor-specific nanoparticle delivery: effect of particle size, Cancer Res. 60 (2000) 4440–4445.

[10] S.V. Vinogradov, T.K. Bronich, A.V. Kabanov, Nanosized cationic hydrogels for drug delivery: preparation, properties and interactions with cells, Adv. Drug Deliv. Rev. 54 (2002) 135–147.

[11] A.E. Hawley, L. Illum, S.S. Davis, The effect of lymphatic oedema on the uptake of colloids to the lymph nodes, Biopharm. Drug Dispos. 19 (1998) 193–197.

[12] P. Serra, P. Santamaria, Nanoparticle-based autoimmune disease therapy, Clin. Immunol. 160 (2015) 3–13.

[13] J. Agudo-Canalejo, R. Lipowsky, Adhesive nanoparticles as local probes of membrane curvature, Nano. Lett. 15 (2015) 7168–7173.

[14] J. Agudo-Canalejo, R. Lipowsky, Critical particle sizes for the engulfment of nanoparticles by membranes and vesicles with bilayer asymmetry, ACS Nano 9 (2015) 3704–3720.

[15] A. Daddi-Moussa-Ider, S. Goh, B. Liebchen, C. Hoell, A.J.T.M. Mathijssen, F. Guzman-Lastra, C. Scholz, A.M. Menzel, H. Lowen, Membrane penetration and trapping of an active particle, J. Chem. Phys. 150 (2019), 064906.

[16] X. Meng, X. Li, Size limit and energy analysis of nanoparticles during wrapping process by membrane, in: Nanomaterials, 8, Basel,, 2018, p. 899.

[17] M.V. Cespedes, Y. Fernandez, U. Unzueta, R. Mendoza, J. Seras-Franzoso, A. Sanchez-Chardi, P. Alamo, V. Toledo-Rubio, N. Ferrer-Miralles, E. Vazquez, S. Schwartz, I. Abasolo, J.L. Corchero, R. Mangues, A. Villaverde, Bacterial mimetics of endocrine secretory granules as immobilized in vivo depots for functional protein drugs, Sci. Rep. 6 (2016) 35765.

[18] J. Seras-Franzoso, C. Diez-Gil, E. Vazquez, E. Garcia-Fruitos, R. Cubarsi, I. Ratera, J. Veciana, A. Villaverde, Bioadhesiveness and efficient mechanotransduction stimuli synergistically provided by bacterial inclusion bodies as scaffolds for tissue engineering, Nanomedicine (Lond.) 7 (2012) 79–93.

[19] J. Seras-Franzoso, K. Peebo, C.J. Luis, P.M. Tsimbouri, U. Unzueta, U. Rinas, M. J. Dalby, E. Vazquez, E. Garcia-Fruitos, A. Villaverde, A nanostructured bacterial bioscaffold for the sustained bottom-up delivery of protein drugs, Nanomedicine. (Lond.) 8 (2013) 1587–1599.

[20] J. Seras-Franzoso, C. Steurer, M. Roldan, M. Vendrell, C. Vidaurre-Agut, A. Tarruella, L. Saldana, N. Vilaboa, M. Parera, E. Elizondo, I. Ratera, N. Ventosa, J. Veciana, A.J. Campillo-Fernandez, E. Garcia-Fruitos, E. Vazquez, A. Villaverde, Functionalization of 3D scaffolds with protein-releasing biomaterials for intracellular delivery, J. Control Release. 171 (2013) 63–72.

[21] J. Seras-Franzoso, K. Peebo, E. Garcia-Fruitos, E. Vazquez, U. Rinas, A. Villaverde, Improving protein delivery of fibroblast growth factor-2 from bacterial inclusion bodies used as cell culture substrates, Acta Biomater. 10 (2014) 1354–1359.

[22] J. Seras-Franzoso, A. Sanchez-Chardi, E. Garcia-Fruitos, E. Vazquez, A. Villaverde, Cellular uptake and intracellular fate of protein releasing bacterial amyloids in mammalian cells, Soft Matter 12 (2016) 3451–3460.

[23] U. Unzueta, M.V. Cespedes, R. Sala, P. Alamo, A. Sanchez-Chardi, M. Pesarrodona, L. Sanchez-Garcia, O. Cano-Garrido, A. Villaverde, E. Vazquez, R. Mangues, J. Seras-Franzoso, Release of targeted protein nanoparticles from functional bacterial amyloids: a death star-like approach, J. Control Release. 279 (2018) 29–39.

[24] E. Vazquez, J.L. Corchero, J.F. Burgueno, J. Seras-Franzoso, A. Kosoy, R. Bosser, R. Mendoza, J.M. Martinez-Lainez, U. Rinas, E. Fernandez, L. Ruiz-Avila, E. Garcia-Fruitos, A. Villaverde, Functional inclusion bodies produced in bacteria as naturally occurring nanopills for advanced cell therapies, Adv. Mater. 24 (2012) 1742–1747.

[25] M. Pesarrodona, T. Jauset, Z.V. Diaz-Riascos, A. Sanchez-Chardi, M.E. Beaulieu, J. Seras-Franzoso, L. Sanchez-Garcia, R. Balta-Foix, S. Mancilla, Y. Fernandez, U. Rinas, S.S. Jr, L. Soucek, A. Villaverde, I. Abasolo, E. Vazquez, Targeting antitumoral proteins to breast cancer by local administration of functional inclusion bodies, Adv. Sci. (Weinh.) 6 (2019), 1900849.

[26] M. Pesarrodona, L. Sanchez-Garcia, J. Seras-Franzoso, A. Sanchez-Chardi, R. Balta-Foix, P. Camara-Sanchez, P. Gener, J.J. Jara, D. Pulido, N. Serna, S.S. Jr, M. Royo, A. Villaverde, I. Abasolo, E. Vazquez, Engineering a nanostructured nucleolin-binding peptide for intracellular drug delivery in triple-negative breast cancer stem cells, ACS Appl. Mater. Interf. 12 (2020) 5381–5388.

[27] U. Unzueta, M.V. Cespedes, N. Ferrer-Miralles, I. Casanova, J. Cedano, J. L. Corchero, J. Domingo-Espin, A. Villaverde, R. Mangues, E. Vazquez, Intracellular CXCR4(+) cell targeting with T22-empowered protein-only nanoparticles, Int. J. Nanomedicine. 7 (2012) 4533–4544.

[28] H. Lopez-Laguna, J. Sanchez, U. Unzueta, R. Mangues, E. Vazquez, A. Villaverde, Divalent cations: a molecular glue for protein, Mater. Trends Biochem. 45 (2020) 992–1003.

[29] H. Lopez-Laguna, U. Unzueta, O. Conchillo-Sole, A. Sanchez-Chardi, M. Pesarrodona, O. Cano-Garrido, E. Volta, L. Sanchez-Garcia, N. Serna, P. Saccardo, R. Mangues, A. Villaverde, E. Vazquez, Assembly of histidine-rich protein materials controlled through divalent cations, Acta Biomater. 83 (2019) 257–264.

[30] J.M. Sanchez, H. Lopez-Laguna, P. Alamo, N. Serna, A. Sanchez-Chardi, V. Nolan, O. Cano-Garrido, I. Casanova, U. Unzueta, E. Vazquez, R. Mangues, A. Villaverde, Artificial inclusion bodies for clinical development, Adv. Sci. (Weinh). 7 (3) (2019), 1902420, https://doi.org/10.1002/advs.201902420 eCollection 2020 Feb.

[31] N. Serna, J.M. Sanchez, U. Unzueta, L. Sanchez-Garcia, A. Sanchez-Chardi, R. Mangues, E. Vazquez, A. Villaverde, Recruiting potent membrane penetrability in tumor cell-targeted protein-only nanoparticles, Nanotechnology. 30 (2019), 115101.

[32] N. Serna, O. Cano-Garrido, J.M. Sanchez, A. Sanchez-Chardi, L. Sanchez-Garcia, H. Lopez-Laguna, E. Fernandez, E. Vazquez, A. Villaverde, Release of functional fibroblast growth factor-2 from artificial inclusion bodies, J. Control Release. 327 (2020) 61–69.

[33] N. Serna, P. Alamo, P. Ramesh, D. Vinokurova, L. Sanchez-Garcia, U. Unzueta, A. Gallardo, M.V. Cespedes, E. Vazquez, A. Villaverde, R. Mangues, J.P. Medema, Nanostructured toxins for the selective destruction of drug-resistant human CXCR4 (+) colorectal cancer stem cells, J. Control Release. 320 (2020) 96–104.

[34] E. Vazquez, M. Roldan, C. Ez-Gil, U. Unzueta, J. Domingo-Espin, J. Cedano, O. Conchillo, I. Ratera, J. Veciana, X. Daura, N. Ferrer-Miralles, A. Villaverde, Protein nanodisk assembling and intracellular trafficking powered by an arginine-rich (R9) peptide, Nanomedicine. (Lond.) 5 (2010) 259–268.

[35] J.L. Corchero, R. Mendoza, J. Lorenzo, V. Rodriguez-Sureda, C. Dominguez, E. Vazquez, N. Ferrer-Miralles, A. Villaverde, Integrated approach to produce a recombinant, His-tagged human alpha-galactosidase A in mammalian cells, Biotechnol. Prog. 27 (2011) 1206–1217.

[36] J.L. Corchero, R. Mendoza, N. Ferrer-Miralles, A. Montràs, L. Martínez, A. Villaverde, Enzymatic characterization of highly stable human alpha-galactosidase A displayed on magnetic particles, Biochem. Eng. J. 67 (2012) 20–27.

[37] R.J. Desnick, K.Y. Allen, S.J. Desnick, M.K. Raman, R.W. Bernlohr, W. Krivit, Fabry's disease: enzymatic diagnosis of hemizygotes and heterozygotes. Alpha-galactosidase activities in plasma, serum, urine, and leukocytes, J. Lab Clin. Med 81 (1973) 157–171.

[38] J.S. Mayes, J.B. Scheerer, R.N. Sifers, M.L. Donaldson, Differential assay for lysosomal alpha-galactosidases in human tissues and its application to Fabry's disease, Clin. Chim. Acta. 112 (1981) 247–251.

[39] V. Sokolova, K. Loza, T. Knuschke, J. Heinen-Weiler, H. Jastrow, M. Hasenberg, J. Buer, A.M. Westendorf, M. Gunzer, M. Epple, A systematic electron microscopic study on the uptake of barium sulphate nano-, submicro-, microparticles by bone marrow-derived phagocytosing cells, Acta Biomater 80 (2018) 352–363.

[40] S. De, D.W. Miller, D.H. Robinson, Effect of particle size of nanospheres and microspheres on the cellular-association and cytotoxicity of paclitaxel in 4T1 cells, Pharm. Res. 22 (2005) 766–775.

[41] S.S. Chakravarthi, S. De, D.W. Miller, D.H. Robinson, Comparison of anti-tumor efficacy of paclitaxel delivered in nano- and microparticles, Int. J. Pharm. 383 (2010) 37–44.

[42] A. Ortiz, D.P. Germain, R.J. Desnick, J. Politei, M. Mauer, A. Burlina, C. Eng, R. J. Hopkin, D. Laney, A. Linhart, S. Waldek, E. Wallace, F. Weidemann, W. R. Wilcox, Fabry disease revisited: management and treatment recommendations for adult patients, Mol. Genet. Metab. 123 (2018) 416–427.

[43] D.P. Germain, P.M. Elliott, B. Falissard, V.V. Fomin, M.J. Hilz, A. Jovanovic, I. Kantola, A. Linhart, R. Mignani, M. Namdar, A. Nowak, J.-P. Oliveira, M. Pieroni, M. Viana-Baptista, C. Wanner, M. Spada, The effect of enzyme replacement therapy on clinical outcomes in male patients with Fabry disease: a systematic literature review by a European panel of experts. Mol. Genet. Metab. Rep. 19 (2019), 100454 https://doi.org/10.1016/j.ymgmr.2019.100454.

[44] L.D. Fialho, V.M. Guimaraes, C.M. Callegari, A.P. Reis, D.S. Barbosa, E.E.D. Borges, M.A. Moreira, S.T. de Rezende, Characterization and biotechnological application of an acid alpha-galactosidase from *Tachigali multijuga* Benth. seeds, Phytochemistry 69 (2008) 2579–2585, wos:000261289600008.

[45] M.Y. Yoon, H.J. Hwang, Reduction of soybean oligosaccharides and properties of alpha-D-galactosidase from *Lactobacillus curvatus* R08 and *Leuconostoc mesenteroides* [corrected] JK55, Food Microbiol. 25 (2008) 815–823.

[46] P.A. Viana, S.T. de Rezende, V.M. Marques, L.M. Trevizano, F.M. Passos, M. G. Oliveira, M.P. Bemquerer, J.S. Oliveira, V.M. Guimaraes, Extracellular alpha-galactosidase from *Debaryomyces hansenii* UFV-1 and its use in the hydrolysis of raffinose oligosaccharides, J. Agric. Food Chem 54 (2006) 2385–2391.

[47] Y. Cao, Y. Wang, H. Luo, P. Shi, K. Meng, Z. Zhou, Z. Zhang, B. Yao, Molecular cloning and expression of a novel protease-resistant GH-36 alpha-galactosidase from *Rhizopus* sp. F78 ACCC 30795, J. Microbiol. Biotechnol. 19 (2009) 1295–1300.

[48] P.V. Bulpin, M.J. Gidley, R. Jeffcoat, D.R. Underwood, Development of a biotechnological process for the modification of galactomannan polymers with plant [alpha]-galactosidase, Carbohydr. Polym. 12 (1990) 155–168.

[49] J. Goldstein, G. Siviglia, R. Hurst, L. Lenny, L. Reich, Group B erythrocytes enzymatically converted to group O survive normally in A, B, and O individuals, Science. 215 (1982) 168–170.

[50] M.L. Olsson, C.A. Hill, L. de V, Q.P. Liu, M.R. Stroud, J. Valdinocci, S. Moon, H. Clausen, M.S. Kruskall, Universal red blood cells–enzymatic conversion of blood group A and B antigens, Transfus. Clin. Biol. 11 (2004) 33–39.

[51] M.L. Olsson, H. Clausen, Modifying the red cell surface: towards an ABO-universal blood supply, Br. J. Haematol. 140 (2008) 3–12.

[52] M.S. Kruskall, J.P. AuBuchon, K.Y. Anthony, L. Herschel, C. Pickard, R. Biehl, M. Horowitz, D.J. Brambilla, M.A. Popovsky, Transfusion to blood group A and O patients of group B RBCs that have been enzymatically converted to group O, Transfusion. 40 (2000) 1290–1298.

[53] A. Zhu, L. Leng, C. Monahan, Z. Zhang, R. Hurst, L. Lenny, J. Goldstein, Characterization of recombinant alpha-galactosidase for use in seroconversion from blood group B to O of human erythrocytes, Arch. Biochem. Biophys. 327 (1996) 324–329.
[54] T. Ito, R. Sadamoto, K. Naruchi, H. Togame, H. Takemoto, H. Kondo, S. Nishimura, Highly oriented recombinant glycosyltransferases: site-specific immobilization of unstable membrane proteins by using Staphylococcus aureus sortase A, Biochemistry. 49 (2010) 2604–2614.
[55] P.C. Lin, S.H. Chen, K.Y. Wang, M.L. Chen, A.K. Adak, J.R. Hwu, Y.J. Chen, C. C. Lin, Fabrication of oriented antibody-conjugated magnetic nanoprobes and their immunoaffinity application, Anal. Chem. 81 (2009) 8774–8782.
[56] W.H. Shao, X.E. Zhang, H. Liu, Z.P. Zhang, A.E. Cass, Anchor-chain molecular system for orientation control in enzyme immobilization, Bioconjug. Chem. 11 (2000) 822–826.
[57] R. Konwarh, D. Kalita, C. Mahanta, M. Mandal, N. Karak, Magnetically recyclable, antimicrobial, and catalytically enhanced polymer-assisted “green” nanosystem-immobilized *Aspergillus niger* amyloglucosidase, Appl. Microbiol. Biotechnol. 87 (2010) 1983–1992.
[58] D.S. Clark, J.E. Bailey, Structure-function relationships in immobilized chymotrypsin catalysis, Biotechnol. Bioeng. 79 (2002) 539–549.